

# Differences in osseointegration rate due to implant surface geometry can be explained by local tissue strains

Craig A. Simmons, Shaker A. Meguid, Robert M. Pilliar \*

*Institute of Biomaterials and Biomedical Engineering and Department of Mechanical and Industrial Engineering, University of Toronto,  
170 College Street, Room 317, Toronto, Ont., Canada M5S 3E3*

Received 16 January 2000; accepted 24 May 2000

## Abstract

Experimental evidence indicates that the surface geometry of bone-interfacing implants influences the nature and rate of tissues formed around implants. In a previously reported animal model study, we showed that non-functional, press-fitted porous-surfaced implants placed in rabbit femoral condyle sites osseointegrated more rapidly than plasma-sprayed implants. We hypothesized that the accelerated osseointegration observed with the porous-surfaced design was the result of this design providing a local mechanical environment that was more favourable for bone formation. In the present study, we tested this hypothesis using finite element analysis and homogenization methods to predict the local strains in the pre-mineralized tissues formed around porous-surfaced and plasma-sprayed implants. We found that, for loading perpendicular to the implant interface, the porous surface structure provided a large region that experienced low distortional and volumetric strains, whereas the plasma-sprayed implant provided little local strain protection to the healing tissue. The strain protected region, which was within the pores of the sintered porous surface layer, corresponded to the region where the difference in the amount of mineralization between the two implant designs was the greatest. Low distortional and volumetric strains are believed to favour osteogenesis, and therefore the model results provide initial support for the hypothesis that the porous-surfaced geometry provides a local mechanical environment that favours more rapid bone formation in certain situations. © 2001 Orthopaedic Research Society. Published by Elsevier Science Ltd. All rights reserved.

## Introduction

The long-term success of bone-interfacing implants for load-bearing orthopaedic and dental applications requires rigid fixation of the implant within the host bone site. This condition, known as functional osseointegration, is achieved in cementless and press-fit implant systems by mechanical interlock between the surface features of the implant (threaded, porous, or textured surfaces) and ingrown bone tissue. Understanding the factors that enhance the potential for osseointegration could improve the design and use of these implant systems, resulting in greater clinical success particularly in situations where osseointegration is typically difficult to achieve.

Earlier in vivo studies have identified implant surface geometry as a design variable that significantly influences long-term implant performance [1,8,10,21,22,33]. We have demonstrated that implant surface geometry also influences the initial healing and mineralization of the tissue in the peri-implant region (the interface zone) [29]. Specifically, we studied the early healing dynamics of the repair/regeneration tissues adjacent to non-functional implants with different surface geometries and demonstrated that implants with a sintered Ti6Al4V porous surface layer osseointegrated more rapidly than Ti plasma-sprayed implants. However, the reason for this differential response was unclear from the experimental studies.

Peri-implant tissue formation and mineralization are dependent on several factors, including the local mechanical environment in the interface zone [26,31]. Carter and Giori [5] suggested that proliferation and differentiation of the mesenchymal cells responsible for peri-implant tissue formation are regulated by the local mechanical environment according to the tissue

\* Corresponding author. Tel.: +1-416-978-1463; fax: +1-416-979-4762.

E-mail address: bob.pilliar@utoronto.ca (R.M. Pilliar).

differentiation hypothesis proposed by Carter and his colleagues for skeletal regeneration [3]. According to Carter's theory, progenitor cells within developing mesenchymal tissues that experience a loading history of low distortional strain and low compressive hydrostatic stress are more likely to become osteogenic, assuming an adequate blood supply. However, if the healing tissue is exposed to excessive distortional strains, fibrogenesis will result. Significant compressive hydrostatic stresses and poor vascularity will result in cartilage or fibrocartilage formation. Based on this hypothesis, one would expect more rapid implant osseointegration when the interface zone tissue experiences minimal distortional strain and hydrostatic stress, as is the case with a stable implant. However, the local mechanical environment around an implant during and after the healing phase is dependent on the forces imposed and the implant surface geometry [16,19,23]. Therefore, certain surface designs may promote osseointegration by providing a favourable local mechanical environment for bone formation. Based on this reasoning, we hypothesized that the accelerated osseointegration observed with non-functional sintered porous-surfaced implants compared with plasma spray-coated implants [29] was the result of the porous-surfaced design, with its characteristic three-dimensional interconnected network of pores, providing a local mechanical environment in the healing tissue that was more favourable for osteogenesis.

The relationship between implant surface geometry, local mechanical environment, and interface tissue formation has not been addressed to date. Previous studies have correlated patterns of peri-implant tissue formation with local mechanical parameters predicted by the finite element method [11,13,27,28], but the models used in those studies did not incorporate the microstructural features of the implant surface and therefore could not account for its influence on the local mechanical environment.

Therefore, our objective was to investigate the effect of implant surface geometry in influencing mechanically regulated tissue formation adjacent to bone-interfacing implants. Using finite element analysis and homogenization theory, we addressed three research questions: (1) what were the effective and local mechanical properties of the interface zones for the porous-surfaced and plasma-sprayed implants used in our previously reported animal experiments [29], (2) what were the local strains in the pre-mineralized interface zone tissue around the porous-surfaced and plasma-sprayed implants in those studies, and (3) do the predictions for local tissue strains, when interpreted within the context of Carter's theory for tissue differentiation, support the hypothesis that the local mechanical environment around the porous-surfaced implants was more conducive to early bone formation compared with the plasma-sprayed implants?

## Materials and methods

### *Review of the experimental model and results*

To determine the effect of implant surface geometry on early tissue healing dynamics, we have characterized the histological and mechanical properties of the healing tissue around non-functional Ti6Al4V sintered porous-surfaced and Ti plasma-sprayed implants [29]. The aspects of the experimental investigation most relevant to the current study are reviewed here.

The implants used were 9 mm long and had a truncated conical (tapered) shape having a taper angle of approximately 5° and a maximum coronal diameter of 4.1 mm. The coronal 1 mm of the implants had a smooth machined surface. As noted previously, the implants were fabricated with one of two bone-interfacing surface geometries: a sintered porous-structured surface or a plasma-sprayed surface. The porous surface was created by sintering Ti6Al4V particles of 45–150 µm in diameter to a machined Ti6Al4V substrate. The resulting porous structure was approximately 225 µm thick (as measured on back-scattered electron micrographs) and consisted of two to three particle layers bonded to each other and the substrate. This treatment produced pore sizes in the range of 50–200 µm, a volume porosity of 35–40%, and a surface region with a three-dimensional interconnected porosity. The plasma-sprayed implants (similar in shape and dimensions to the porous-surfaced design) were produced by application of a titanium plasma spray coating to a machined Ti6Al4V substrate. The plasma-sprayed layer had an average thickness of 20–25 µm (measured on back-scattered electron micrographs). This treatment produced a rough, irregular surface with approximately 5–10% volume porosity. Unlike the interconnected network of pores and channels observed with the sintered porous-surfaced structure, the pores within the layer were more or less isolated. However, the plasma-sprayed surface did possess regions with undercuts and intrusions that permitted interdigitation and mechanical interlock with tissue.

The implants were inserted transversely in the medial femoral condyles of 21 New Zealand White rabbits (with each rabbit receiving one implant of each design) and the implant–tissue interface zones were evaluated histologically and mechanically at 0, 4, 8 and 16 days post-implantation. The implants were placed with the porous and plasma-sprayed surface regions in cancellous bone. The implants were not loaded directly, although load transfer through the condyles to the implant interface was expected.

Histological analysis and scanning electron microscopy demonstrated a well-defined interface zone adjacent to both implant designs 4 days post-implantation, with more extensive integration of the healing tissue with the sintered porous surface, but no evidence of mineralization with either implant design. Eight days post-implantation, back-scattered electron micrographs demonstrated areas of localized bone formation within the pores and adjacent to the sintered particles of the porous-surfaced region, whereas there was no evidence of mineralized tissue juxtaposed to the plasma-sprayed coating. Thus, mineralization leading to osseointegration occurred more rapidly with the porous-surfaced implants. As a result of the more extensive tissue integration and more rapid matrix mineralization, the porous-surfaced implants were more strongly attached and exhibited higher interfacial stiffnesses 4 and 8 days post-implantation. Sixteen days post-implantation, both implant designs were more or less fully osseointegrated and had comparable attachment characteristics.

In order to quantify our previous observations of more extensive mineralization with the porous-surfaced implants, we determined the mineralized area within the interface zones of the two implant designs 8 days post-implantation. Digital back-scattered electron micrographs were thresholded using SigmaScan (SPSS, Chicago, IL) to identify mineralized tissue, and the total mineralized area was measured within the surface structure region and within the region adjacent to the surface structure for the two implant designs. In the original study, the implants from two rabbits were assigned for examination by back-scattered electron microscopy. Two to four sections of each implant from these two rabbits were analyzed to determine the average mineralized areas. Since each rabbit had one implant of each design, we compared the results for the two implant designs on a pairwise basis.

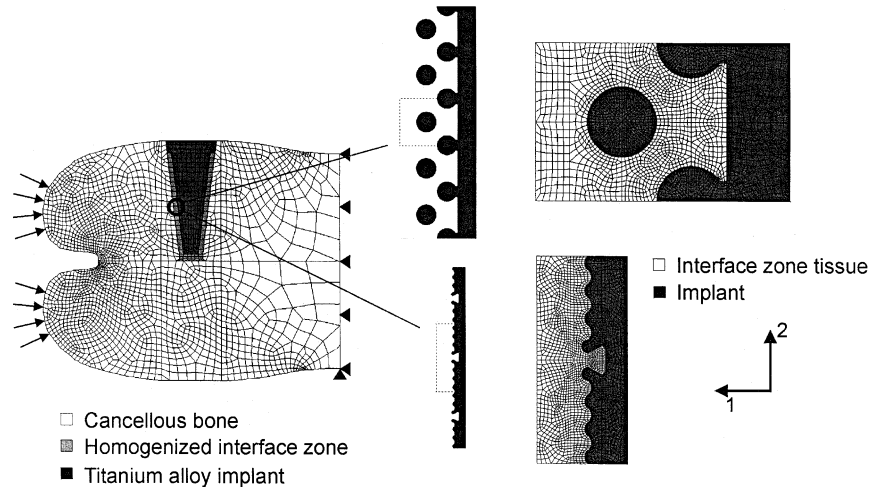


Fig. 1. Two-dimensional, plane stress finite element models of the whole implant and unit cells with idealized geometries representing the porous-surfaced (top) and plasma-sprayed (bottom) designs. The global model, porous-surfaced unit cell, and plasma-sprayed unit cell had 2400, 2228, and 2468 four-noded elements, respectively. Penalty constraints were applied to the porous-surfaced unit cell model to prevent relative displacement of the metal components with respect to one another, thus simulating the relative stiffness of the surface structure. The unit cell models were analyzed using homogenization theory with periodic boundary conditions. The width of the interface zone in the global models was 367  $\mu\text{m}$  for the porous-surfaced implant and 133  $\mu\text{m}$  for the plasma-sprayed implant.

#### Computational model

We used the finite element method and homogenization theory to predict the local strains in the healing interface zone following implantation of sintered porous-surfaced and plasma-sprayed implants. The homogenization approach was selected because it permitted incorporation of the microstructural features of the implant interface into a global model of the entire implant, as described below. Previous studies have demonstrated the suitability of this method for studying tissue-implant interface mechanics [15–17].

Homogenization theory is a mathematical tool that has been used to analyze the effective and local mechanical behaviours of composite materials with a periodic microstructure [30]. A detailed presentation of the theory and its implementation has been reported by Hollister and Kikuchi [12]. The two key assumptions in this theory are that the microstructure is spatially periodic and the field variables vary both on the global scale (as in standard continuum analyses) and on the local scale due to the heterogeneity in the microstructure. Based on these assumptions, the composite being analyzed can be modelled by a series of repeating unit cells (UCs) that are representative of the microstructure. The homogenization method decouples the analysis of the composite into analyses at the local (microscopic) and global (macroscopic) levels. The local level analysis of the UC provides the effective stiffness tensor of the composite,  $\bar{C}_{ijkl}$ , and the local structure tensor,  $M_{ijkl}$ . The effective stiffness tensor describes the properties of the composite on the global level and can be used to predict the average strains acting in the composite. The local structure tensor maps the average strain in the composite to the local strain field within the unit cell. This formulation was implemented numerically using a custom software package written using MATLAB (The Mathworks, Natick, MA) in conjunction with a commercial finite element package (ANSYS 5.4, Ansys, Canonsburg, PA).

Unit cell and global finite element models of the sintered porous-surfaced and plasma spray-coated implants 4 days post-implantation were developed. After this short period of healing, a well-defined interface zone filled with early repair tissue had formed adjacent to both implant designs, but without any evidence of mineralization [29]. The porous-surfaced and plasma-sprayed interface zones (composites of the implant surface features and loosely organized granulation tissue) were modelled by a series of repeating unit cells (Fig. 1). The UCs had idealized geometries that were based on the characteristics of the two surface designs used in the experiments, including volume porosity, pore size, interface zone width, and allowance for mechanical interlock between the tissue and implant surface features. The implant material

Table 1

Elastic constants used in the finite element models

Material	Elastic modulus, $E$	Poisson's ratio, $\nu$
Titanium	110 (GPa)	0.33
Trabecular bone <sup>a</sup>	500 (MPa)	0.4
Interface zone tissue <sup>b</sup>	1 (MPa)	0.45
Homogeneous interface zone	Determined by homogenization analysis	

<sup>a</sup> Based on representative values from Keaveny and Hayes [14].

<sup>b</sup> The elastic properties of the interface zone tissue were similar to those of the initial tissues formed during fracture healing [4,6,7].

and ingrown tissue were modelled as homogeneous, linear elastic materials with the properties given in Table 1. It was assumed that the metal and tissue were perfectly bonded and that the tissue infiltrated the porosity or irregularities of the implant surfaces fully.

Two-dimensional, plane stress global finite element models were developed to represent the tapered implant placed transversely in the trabecular bone of the rabbit femoral condyle (Fig. 1). All materials were modelled as homogeneous and linear elastic (Table 1). The global models for the two implant surface designs were identical, except for the width of the homogenized interface zone. Although the implants were not loaded during the experiment, the rabbits ambulated shortly after implantation, thereby loading their femoral condyles and consequently the implants and concomitant interface zone tissues. Uniform compressive pressure loads (1.5 MPa) were applied normal to each condylar surface; this loading condition is representative of the largest load experienced in vivo [20].

Based on the finite element and homogenization analyses, the effective elastic constants ( $\bar{C}_{ijkl}$ ) and local structure tensor ( $M_{ijkl}$ ) were determined for each surface design. The effective elastic constants were used to describe the properties of the homogenized interface zone, and the average tissue strain tensors ( $\bar{\epsilon}_{kl}$ ) were determined at a mid-length location for each design by finite element analysis of the global model. The local tissue strains within the unit cells ( $\epsilon_{ij}$ ) at this location were then determined from the average tissue strains and the local structure tensors according to  $\epsilon_{ij} = M_{ijkl}\bar{\epsilon}_{kl}$ . The local tissue strains were expressed as the distortional (octahedral) tissue strain,

$$\varepsilon_{\text{dist}} = \frac{1}{3} \left[ (\varepsilon_1 - \varepsilon_2)^2 + (\varepsilon_2 - \varepsilon_3)^2 + (\varepsilon_3 - \varepsilon_1)^2 \right]^{1/2},$$

and the volumetric tissue strain (related to the hydrostatic stress),

$$\varepsilon_{\text{vol}} = \frac{1}{3} (\varepsilon_1 + \varepsilon_2 + \varepsilon_3),$$

where  $\varepsilon_1$ ,  $\varepsilon_2$ , and  $\varepsilon_3$  are the principal strains. Comparisons were made between the two implant surface designs and interpreted according to Carter's tissue differentiation hypothesis [3].

## Results

### Mineralized area

Based on quantitative analysis of the back-scattered electron micrographs, there was more mineralized tissue within the pores of the sintered porous surface than within the irregularities of the plasma-sprayed coating. In the region outside the surface structure, however, the differences between the implant designs were less marked. In rabbit #1, there was 27.5 times more mineralized area in the sintered porous surface layer than in the plasma-sprayed layer, but only 4.9 times more mineralized area in the adjacent region. Similarly, in rabbit #2 the ratio of the porous-surfaced mineralized area to that of the plasma-sprayed implant was 10.8 in the surface layer and 1.4 in the adjacent region.

### Effective properties of the interface zones

The effective elastic constants of the homogenized interface zones were highly anisotropic. In the direction parallel to the long axis of the implant, the modulus was dominated by the stiffness of the metal substrate and surface structure, whereas normal to the implant surface the modulus was dictated primarily by the compliance of the tissue component (Table 2). Compared to the plasma-sprayed interface zone, the perpendicular and shear moduli for the porous-surfaced interface zone were over 57% larger. Since load transfer to the implant interface during the animal experiments was primarily perpendicular to the implant interface, the properties perpendicular to the interface and in shear would be expected to dominate the local mechanical environment.

Table 2  
Effective elastic constants of the interface zones predicted by homogenization analysis<sup>a</sup>

Component	Porous-surfaced	Plasma-sprayed
$E_1$ (MPa)	3.59	2.29
$E_2$ (GPa)	28.2	31.3
$G_{12}$ (MPa)	1.18	0.663
$\nu_{12}$	$3.9 \times 10^{-5}$	$2.5 \times 10^{-5}$
$\nu_{21}$	0.306	0.348

<sup>a</sup>Directions 1 and 2 are perpendicular and parallel to the implant interface, respectively.

### Local properties of the interface zones

Due to the local surface geometry, the porous-surfaced interface zone had large regions within the pores of the surface structure that were "strain protected", particularly for the components of the local structure tensor perpendicular to the implant interface ( $M_{1111}$ ) and in shear ( $M_{1212}$ ) (Fig. 2). Although the tissue within the pores of the plasma-sprayed coating was similarly protected, this amount of tissue represented only a small area. For both implant designs, the tissue in the region outside the surface structure had higher magnitudes of the local structure components  $M_{1111}$  and  $M_{1212}$ , with higher magnitudes for the porous-surfaced interface zone.

### Local tissue strains

Due to stiffer effective properties and local strain shielding, the tissue strains around the porous-surfaced implant were generally lower, particularly within the pores of the surface structure (Fig. 3). For instance, 85%

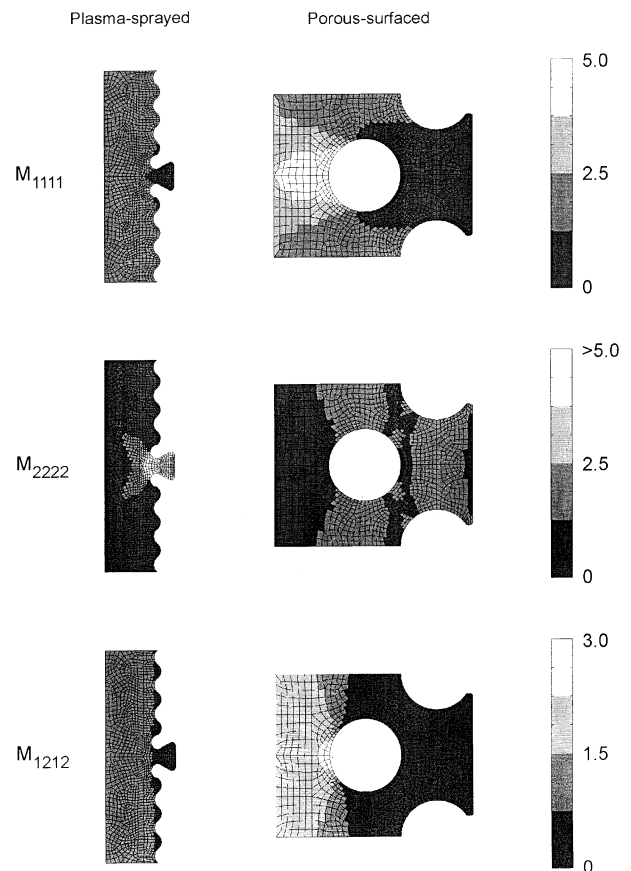


Fig. 2. Field plots of the local structure tensor components for the porous-surfaced interface zone tissue (right) and plasma-sprayed interface zone tissue (left). From top to bottom, the components shown are the component normal to the implant interface ( $M_{1111}$ ), parallel to the implant interface ( $M_{2222}$ ), and in shear ( $M_{1212}$ ).

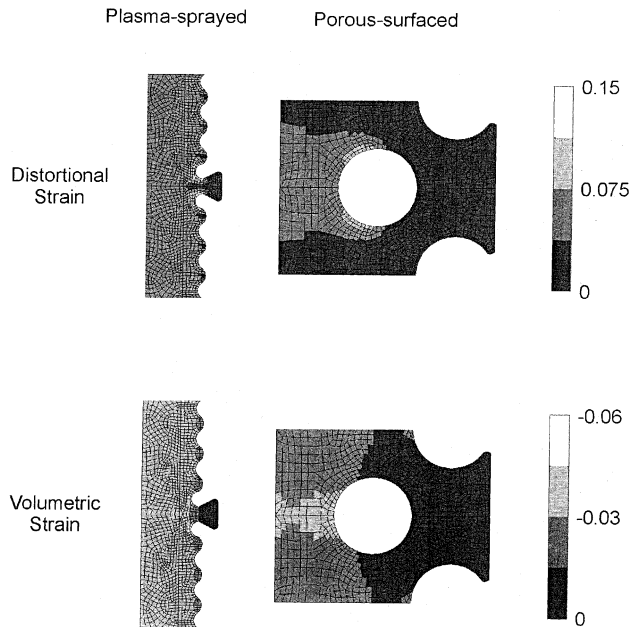


Fig. 3. Field plots of the local distortional and volumetric tissue strains for the plasma-sprayed (left) and porous-surfaced (right) surface geometries. Dark areas are regions with low strain magnitudes, whereas light areas are regions with high strain magnitudes. Generally, the majority of tissue in the porous-surfaced interface zone experienced lower strain levels than the tissue in the plasma-sprayed interface zone.

of the tissue in the porous-surfaced interface zone experienced distortional strains lower than the median distortional strain in the plasma-sprayed interface zone tissue. Similarly, the volumetric strain magnitude in over 99% of the porous-surfaced interface zone tissue was lower than the median value for the plasma-sprayed interface zone tissue (Fig. 4).

## Discussion

In an earlier study, we observed more rapid mineralization of the interface tissue around non-functional porous-surfaced implants compared with plasma-sprayed implants [29]. The more rapid osseointegration appeared to result from greater localized bone formation within the pores and adjacent to the surface of the porous-surfaced implants. We hypothesized that this differential response was because the surface geometry of the porous-surfaced implants provided a local mechanical environment that was more favourable for bone formation. The objective of the current study was to test this hypothesis using finite element analysis and homogenization theory to predict the local tissue strains before mineralization around the two implant surface designs used in the animal experiments. For loading perpendicular to the implant interface, we found that the porous surface structure provided an interface zone with stiffer effective properties and larger strain pro-

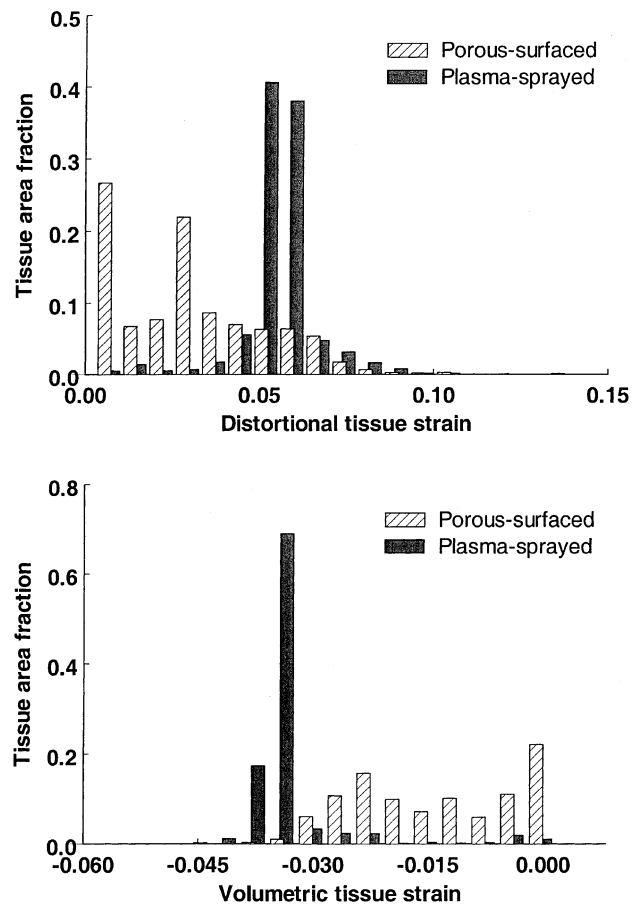


Fig. 4. Histograms illustrating the area fraction of tissue experiencing various levels of distortional and volumetric strain for the two implant surface designs. The “strain protected” region of the porous-surfaced interface zone is evident in both cases.

ected regions than did the plasma-sprayed coating. As a result, the distortional and volumetric tissue strains were generally lower around the porous-surfaced implant, and particularly within the pores of the surface layer, the region where the differences in amount of mineralization between the two implant designs were the greatest. Lower distortional and volumetric tissue strains favour bone formation according to Carter’s tissue differentiation theory [3], and therefore the modelling results provide initial support for our hypothesis that, for the case considered here, the porous-surfaced geometry provides a local mechanical environment that is favourable for more rapid bone formation.

Our analysis suggests that the advantage of the porous-surfaced design over the plasma-sprayed design is that it provides a greater area in which the healing tissue is strain protected, permitting more rapid osteogenesis in those areas. Our analysis considered a single time point, representing the period prior to tissue mineralization. In this study, we did not attempt to develop a dynamic quantitative regulatory model relating the mechanical parameters to tissue synthesis; such a model

would require experimental data relating well-defined loading conditions with tissue formation, and the loading conditions used in this study and others [13,28] were based on gait analysis, and therefore are only approximate values. Nonetheless, a qualitative description of the tissue formation process and its relationship to the local mechanical environment can be postulated from our analyses.

Assuming that low distortional and volumetric strains favour bone formation, the model results predict more bone formation in the porous-surfaced interface zone. With mineralization of the porous-surfaced interface zone tissue, the effective stiffness of the interface zone would increase and more regions may become strain protected. Thus, assuming the applied loads did not change, the local mechanical environment would become more favourable for further bone formation, resulting in an increased rate of mineralization until the implant is osseointegrated. The plasma-sprayed interface zone starts with a less favourable environment for bone formation (fewer regions of low distortional and volumetric strains). However, as mineralization occurred at some preferred sites, the local strains would decrease. This change in local strain magnitudes would develop slowly at first and more rapidly as tissue mineralization and stiffening progressed. Thus, the tissues within the porous-surfaced interface zone would mineralize rapidly from the start, whereas the rate of mineralization in the plasma-sprayed interface zone would be slow initially, but would accelerate as mineralization occurred. This pattern of healing is consistent with that observed in our previously reported rabbit model experiments [29] and is similar to that proposed by Perren and Cordey [24] for fracture healing and by Prendergast et al. [28] for peri-implant tissue formation. Our image analysis also demonstrated that bone formation occurred outside the protected regions of the implant surface structures, in regions with higher strains. The new bone formed in this region was not localized, but adjoined the existing host bone surfaces, suggesting that the regulation of appositional bone formation may be governed by other factors, both mechanical (as suggested by Claes and Heigele [7]) and non-mechanical.

Previous finite element studies have examined the relationship between mechanical stimuli and peri-implant tissue formation at the tissue-implant [13,27,28] and tissue-cement interfaces [11]. These studies did not account for the geometric features of the implant surface even though *in vivo* studies have shown that implant surface geometry significantly influences the initial healing response [29] and long-term implant performance [1,8,10,21,22,33]. Therefore, we used a unit cell modelling approach to incorporate the geometric characteristics of the implant surfaces into global models of the whole implant systematically and efficiently. The significant influence of the surface geometry on the local

mechanical environment was evident from the model predictions. The local level analyses revealed that the interface zone tissue experiences a range of strain magnitudes due to the microstructural surface features. For instance, the magnitudes of the local distortional strains in the porous-surfaced interface zone ranged from 5% to 807% of the magnitude of the global distortional strain at the same location.

Although the homogenization approach was necessary to incorporate implant surface geometry into the models, the approach required several assumptions to be made. Two key conditions in homogenization theory are that the microstructure is spatially periodic and can be represented by repeating unit cells. Clearly, neither condition is met completely by the tissue-implant interface zone. Although the interface zone, as modelled in this study, was periodic only in the direction parallel to the implant interface, the homogenization approach has been shown to be accurate for loads applied either parallel or perpendicular to the direction of periodicity (as was the case in this study) [15,18]. The unit cell models we developed for the two implant surface designs were based on key characteristics of the actual surfaces, but clearly do not represent accurately the real surface geometries, which are heterogeneous and therefore not modelled readily by a single representative unit cell. The idealization of the geometries would likely limit the accuracy with which predictions can be made, particularly for the absolute magnitudes and spatial distributions of the local tissue strains. Nonetheless, the unit cell geometries capture the essential features of the surface designs and therefore are sufficient for an initial understanding of the relative differences between the designs.

In addition to the assumptions on the unit cell geometry, we made assumptions on the mechanical behaviour of the tissue and its interaction with the implant surface. For all materials, we used single-phase, isotropic, linear elastic material models. While this is accurate for the metal and trabecular bone in the global level analysis, a poroelastic [28] or hyperelastic [11] material model may be more appropriate for the early interface zone tissue. However, the mechanical behaviour of early interface zone tissue is poorly characterized, and therefore it is difficult to determine the most appropriate material description. The elastic properties we used for the interface tissue were similar to those of the initial tissues formed during fracture healing [4,6,7]. We were also limited in our selection of a material model by the homogenization method, which is most readily implemented numerically with linear elastic material descriptions for the composite components. Because our primary research objective was to investigate surface geometry effects, we used a modelling approach that considered local geometry effects at the expense of a more accurate material model. Had the tissue been modelled as a poroelastic or hyperelastic material, we

would expect similar differences between the two designs. Recently, Wu et al. [34] incorporated biphasic material descriptions into homogenization schemes to study cartilage mechanics; this work provides a theoretical basis for the development of biphasic micromechanical models of the tissue–implant interface.

The other assumption we made regarding the interface zone tissue was that it was rigidly bonded to the metal surfaces of the implant interface. As with the material properties of the interface tissue, the mechanical characteristics of the interface between the tissue and implant surface are not well characterized. Microscopic examination of the tissue–implant interface indicates that one of the first events in the healing process is the formation of a collagen-free calcified tissue layer at the implant interface [9]. This layer is not chemically bonded to the titanium alloy surface, but is likely attached mechanically by interdigitation with submicron features on the surface (e.g., ridges due to machining or thermal etching lines formed during sintering of Ti alloy particles [25]). Therefore, a weak interface bond may exist at the tissue–implant interface, consistent with our model assumption. Currently, numerical implementation of the homogenization method is limited to bonded or slip interface conditions [17], and therefore our model cannot account for debonding of the tissue from the interface, which may occur *in vivo*.

We interpreted our results in terms of the tissue differentiation hypothesis proposed by Carter and co-workers [3], in which the mechanical parameters controlling tissue formation are distortional and volumetric strain (or hydrostatic stress). This model is well suited for analyses with single-phase materials. We have taken some liberties in our interpretation of the model by suggesting the *rate* of tissue formation is dependent on the strain invariants. This seems reasonable, since it is unlikely that the formation of various skeletal tissues is delimited by distinct threshold strain values. Prendergast et al. [28] proposed a different model in which peri-implant tissue formation was dictated by distortional tissue strain and the velocity of the fluid within the tissue relative to the solid phase. In order to incorporate fluid and solid components, a biphasic material model was used for the interface zone tissue. We were limited to a single-phase material model for the tissue, since incorporating a biphasic model into the homogenization scheme was not feasible, and therefore we interpreted our results using Carter's tissue differentiation hypothesis. The appropriateness of a single-phase versus a biphasic material model and the implications to the various tissue differentiation theories were recently debated [2,32]. However, until the specific details and mechanisms of mechanical regulation of tissue formation are revealed by well-formulated cell and tissue culture studies, arguments regarding the most appropriate model for tissue formation are based on specu-

lation and circumstantial evidence. Despite possible limitations to Carter's model, the success with which it has been applied previously suggests that it is adequate for a general understanding of how skeletal tissue formation is influenced by mechanical stimuli.

In conclusion, our computational analyses suggested that in cases where loading is normal to the implant interface, the porous-surface geometry provided a local mechanical environment that was more favourable for localized bone formation than that provided by the plasma-sprayed surface design. This finding provides an explanation for the more extensive and accelerated osseointegration we observed previously with porous-surfaced implants. The issues of microstructure and its effect on local mechanical environment and tissue formation are important not only to the design of bone-interfacing implants, but also to the design of tissue engineering scaffolds, where appropriate control of tissue formation is essential to engineer functional tissues.

### Acknowledgements

This work was supported by the Medical Research Council of Canada.

### References

- [1] Buser D, Schenk RK, Steinemann S, Fiorellini JP, Fox CH, Stich H. Influence of surface characteristics on bone integration of titanium implants. A histomorphometric study in miniature pigs. *J Biomed Mater Res* 1991;25:889–902.
- [2] Carter DR, Beaupré GS. Linear elastic and poroelastic models of cartilage can produce comparable stress results: a comment on Tanck et al. (*J Biomech* 1999;32:153–61). *J Biomech* 1999; 32:1255–6.
- [3] Carter DR, Beaupre GS, Giori NJ, Helms JA. Mechanobiology of skeletal regeneration. *Clin Orthop* 1998;355(Suppl):S41–55.
- [4] Carter DR, Blenman PR, Beaupré GS. Correlations between mechanical stress history and tissue differentiation in initial fracture healing. *J Orthop Res* 1988;6:736–48.
- [5] Carter DR, Giori NJ. Effect of mechanical stress on tissue differentiation in the bony implant bed. In: Davies JE, editor. *The bone-biomaterial interface*. Toronto: University of Toronto Press; 1991. p. 367–79.
- [6] Cheal EJ, Mansmann KA, DiGioia AM, Hayes WC, Perren SM. Role of interfragmentary strain in fracture healing: Ovine model of a healing osseotomy. *J Orthop Res* 1991;9:131–42.
- [7] Claes LE, Heigele CA. Magnitudes of local stress and strain along bony surfaces predict the course and type of fracture healing. *J Biomech* 1999;32:255–66.
- [8] Cochran DL, Schenk RK, Lussi A, Higginbottom FL, Buser D. Bone response to unloaded and loaded titanium implants with a sandblasted and acid-etched surface: a histometric study in the canine mandible. *J Biomed Mater Res* 1998;40:1–11.
- [9] Davies JE. *In vitro* modeling of the bone/implant interface. *Anat Record* 1996;25:426–45.
- [10] Friedman RJ, An YH, Ming J, Draughn RA, Bauer TW. Influence of biomaterial surface texture on bone ingrowth in the rabbit femur. *J Orthop Res* 1996;14:455–64.

- [11] Giori NJ, Ryd L, Carter DR. Mechanical influences on tissue differentiation at bone–cement interfaces. *J Arthroplasty* 1995; 10:514–22.
- [12] Hollister SJ, Kikuchi N. A comparison of homogenization and standard mechanics analyses for periodic porous composites. *Comput Mech* 1992;10:73–95.
- [13] Huiskes R, Driel WDV, Prendergast PJ, Søballe K. A biomechanical regulatory model for periprosthetic fibrous-tissue differentiation. *J Mater Sci: Mats in Med* 1997;8:785–8.
- [14] Keaveny TM, Hayes WC. Mechanical properties of cortical and trabecular bone. In: Hall BK, editor. *Bone*. Boca Raton: CRC Press; 1993. p. 285–344.
- [15] Ko C-C. Mechanical characteristics of implant/tissue interphases. Ph.D. Thesis, University of Michigan, 1994.
- [16] Ko CC, Kohn DH, Hollister SJ. Micromechanics of implant/tissue interfaces. *J Oral Impl* 1992;18:220–30.
- [17] Ko C-C, Kohn DH, Hollister SJ. Effective anisotropic elastic constants of bimaterial interphases: comparison between experimental and analytical techniques. *J Mater Sci: Mats in Med* 1996;7:109–17.
- [18] Kohn DH, Ko C-C, Hollister SJ. Coupled global/local modeling of porous coated implants: error estimates for different loading conditions. *Trans Orthop Res Soc* 1993;39:469.
- [19] Kohn DH, Ko C-C, Hollister SJ. Effect of tissue modulus, symmetry and fibrous tissue on the local properties of a porous coating/tissue interfacial zone. *Trans Orthop Res Soc* 1993;39:223.
- [20] Lerner A. Influence of mechanical stresses on normal bone growth in the developing femur. Ph.D. Thesis, University of Michigan, 1996.
- [21] Luckey HA, Lamprecht EG, Walt MJ. Bone apposition to plasma-sprayed cobalt-chromium alloy. *J Biomed Mater Res* 1992;26:557–75.
- [22] Maniopoulos C, Pilliar RM, Smith DC. Threaded versus porous-surfaced designs for implant stabilization in bone-endodontic implant model. *J Biomed Mater Res* 1986;20:1309–33.
- [23] Pedersen DR, Brown TD, Brand RA. Interstitial bone stress distributions accompanying ingrowth of a screen-like prosthesis anchorage layer. *J Biomech* 1991;24:1131–42.
- [24] Perren SM, Cordey J. The concept of interfragmentary strain. In: Uthoff HK, editor. *Current concepts of internal fixation of fractures*. New York: Springer; 1980. p. 63–77.
- [25] Pilliar RM. Porous-surface metallic implants for orthopaedic applications. *J Biomed Mater Res* 1987;21:1–33.
- [26] Pilliar RM. Quantitative evaluation of the effect of movement at a porous coated implant–bone interface. In: Davies JE, editor. *The bone–biomaterial interface*. Toronto: University of Toronto Press; 1991. p. 380–87.
- [27] Prendergast PJ, Huiskes R. Finite element analysis of fibrous tissue morphogenesis – A study of the osteogenic index with a biphasic approach. *Mech Comput Mater* 1996;32:144–50.
- [28] Prendergast PJ, Huiskes R, Søballe K. Biophysical stimuli on cells during tissue differentiation at implant interfaces. *J Biomech* 1997;30:539–48.
- [29] Simmons CA, Valiquette N, Pilliar RM. Osseointegration of sintered porous-surfaced and plasma-spray coated implants: an animal model study of early post-implantation healing response and mechanical stability. *J Biomed Mater Res* 1999; 47:127–38.
- [30] Suquet PM. Elements of homogenization for inelastic solid mechanics. In: Sanchez-Palencia E, Zaoui A, editors. *Homogenization techniques for composite media*. New York: Springer; 1985. p. 194–278.
- [31] Szmukler-Moncler S, Salama H, Reingewirtz Y, Dubruille JH. Timing of loading and effect of micromotion on bone–dental implant interface: review of experimental literature. *J Biomed Mater Res (Appl Biomater)* 1998;43:192–203.
- [32] Tanck E, van Driel WD, Blankevoort L, Huiskes R, Hagen JW, Burger EH. Response to Beaupré and Carter. *J Biomech* 1999;32:1257.
- [33] Thomas KA, Cook SD. An evaluation of variables influencing implant fixation by direct bone apposition. *J Biomed Mater Res* 1985;19:875–901.
- [34] Wu JZ, Herzog W, Epstein M. Modelling of location- and time-dependent deformation of chondrocytes during cartilage loading. *J Biomech* 1999;32:563–72.